Supporting Information

The Future is Garbage: Repurposing of food waste to an integrated biorefinery

Elvis Ebikade[1,2], Abhay Athaley[1,3], Benjamin Fisher[2], Kai Yang[4,5], Changqing Wu[5], Marianthi G. Ierapetritou,[1,2] and Dionisios G. Vlachos[1,2]*

[1]Catalysis Center for Energy Innovation, University of Delaware, 221 Academy Street, Newark, DE, 19716 USA.

[2]Department of Chemical and Biomolecular Engineering, University of Delaware, 150 Academy Street, Newark, DE, 19716 USA.

[3]Department of Chemical and Biochemical Engineering, Rutgers, The State University of New Jersey, 98 Brett Rd, Piscataway, NJ 08854 (USA)

[4]Department of Food Science and Technology, Zhejiang University of Technology, 866 Yuhangtang Road, Hangzhou 310014, P. R. china

[5]Department of Animal and Food Sciences, University of Delaware, 531 S College Ave, Newark, DE, 19716 USA

**Corresponding author: vlachos@udel.edu*

The SI contains 17 pages, 16 Tables, and 15 Figures.

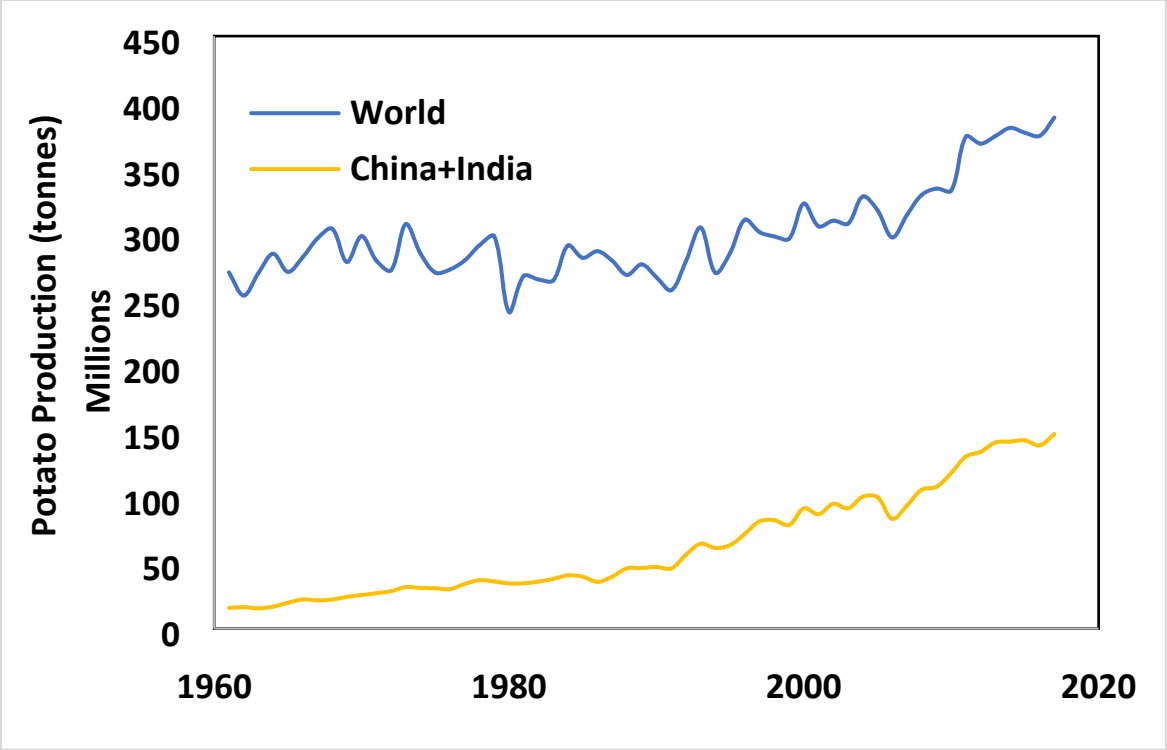

Figure S1. Potato production from 1960 – 2017, globally and in China + India.[1]

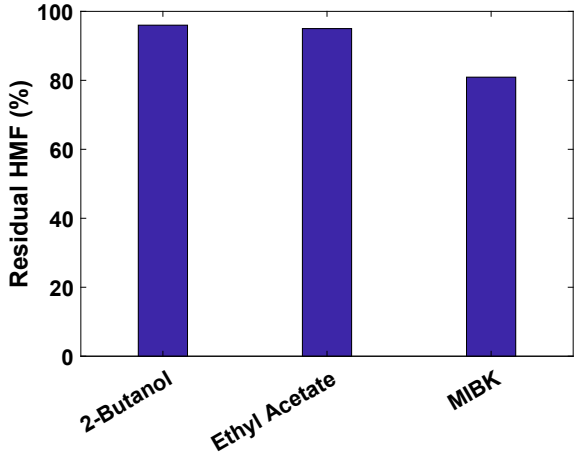

Figure S2. Reactivity study of organic solvents with HMF. Metric to indicate the extent to which HMF is degraded on heating in various organic solvents.

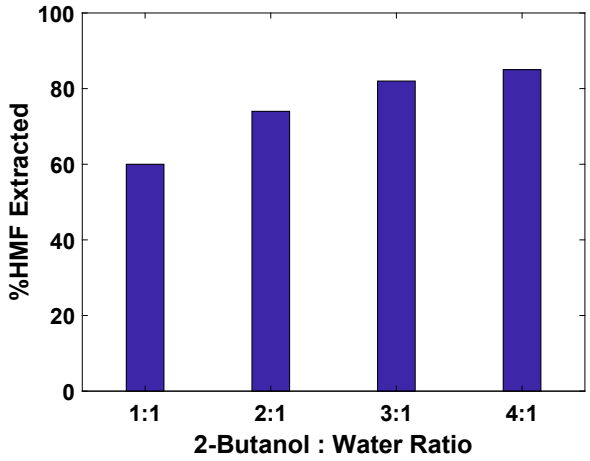

Figure S3. Effect of solvent:water ratio on fraction of HMF extracted. Partition studies using 1 ml of 1 wt. % HMF in 25 wt. % LiBr + 0.05 M H_2SO_4 as aqueous phase.

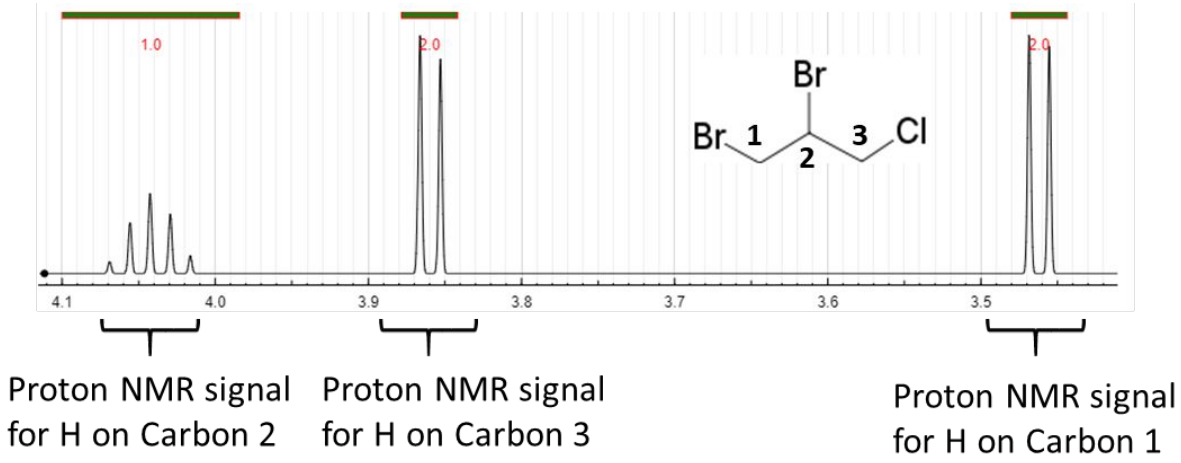

Figure S4. H-NMR signals for DBCP.

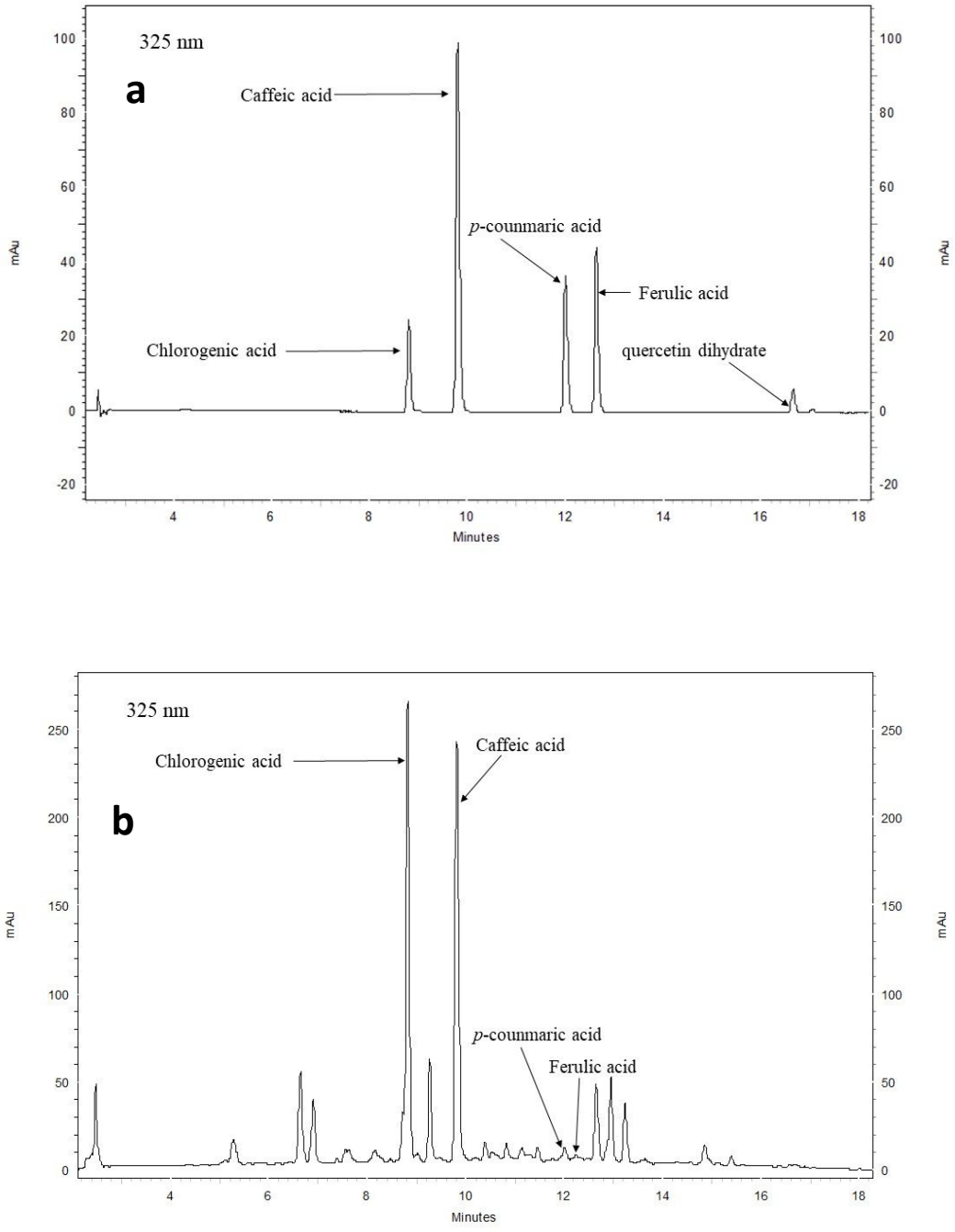

Figure S5. Chromatogram of standards (a) and PPW extracts (b).

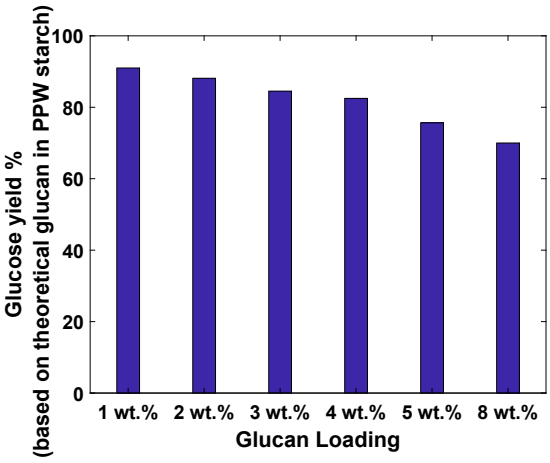

Figure S6. Effect of feedstock loading on glucose yield.

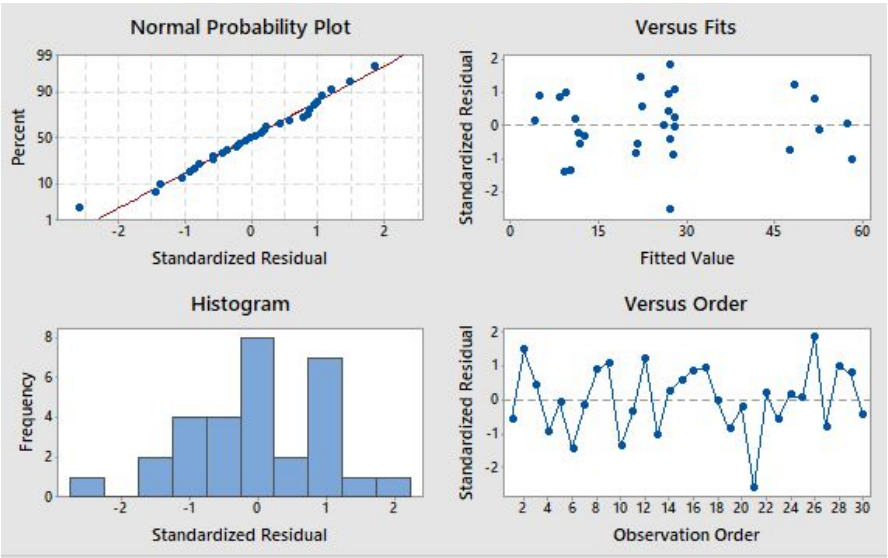

Figure S7. Residual plots for HMF yield.

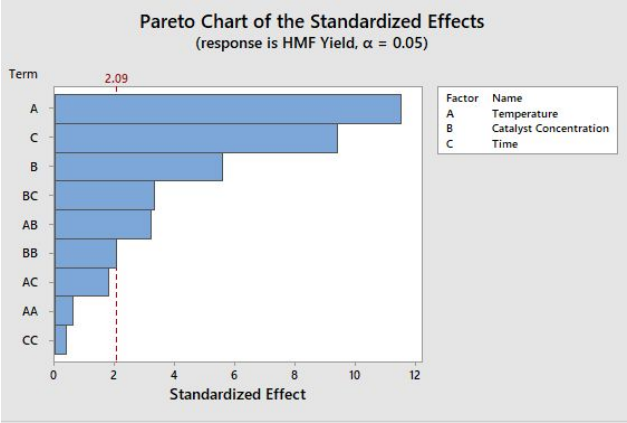

Figure S8. Pareto chart of standardized effects on HMF yield.

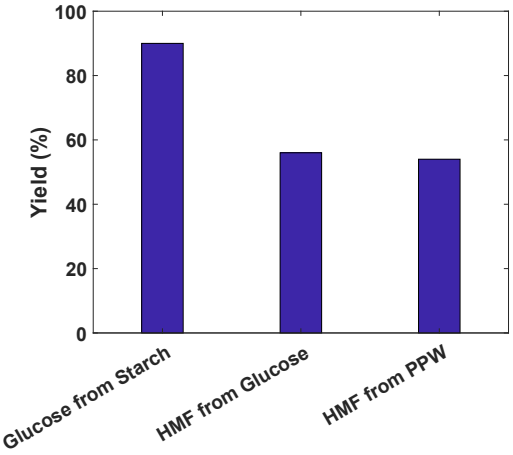

Figure S9. Starch conversion to glucose and HMF yield from starch and PPW.

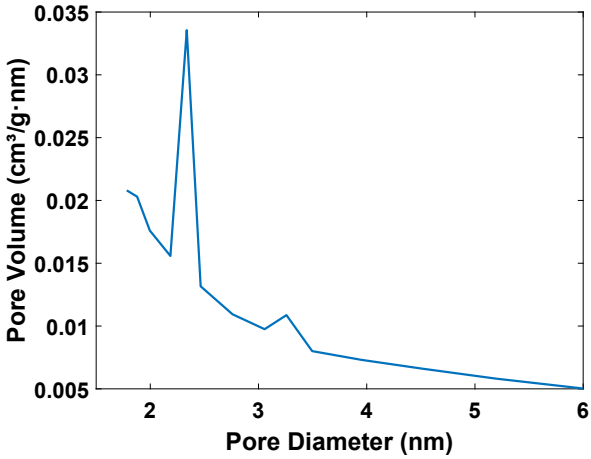

Figure S10. Pore size distribution of PPW residue biochar.

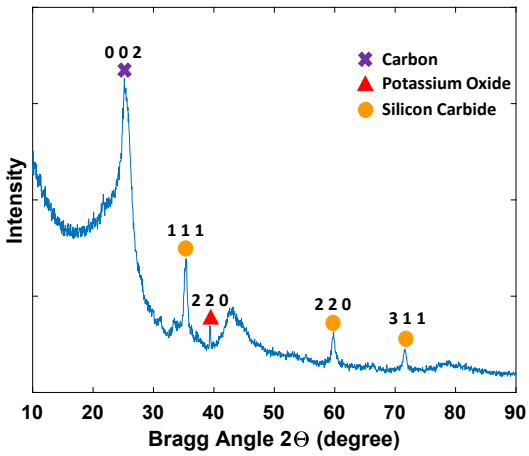

Figure S11. XRD of PPW biochar.

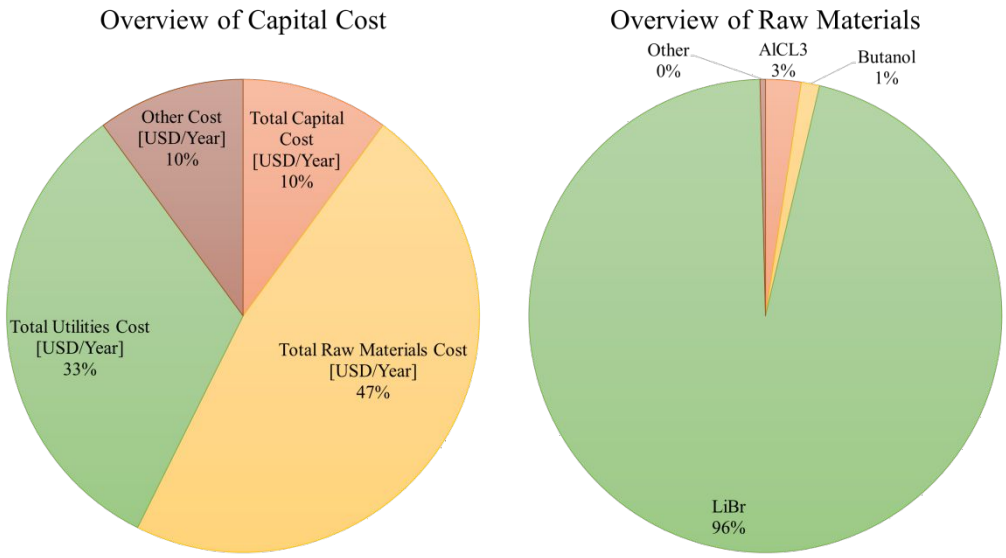

Figure S12. Breakdown of capital and raw material cost.

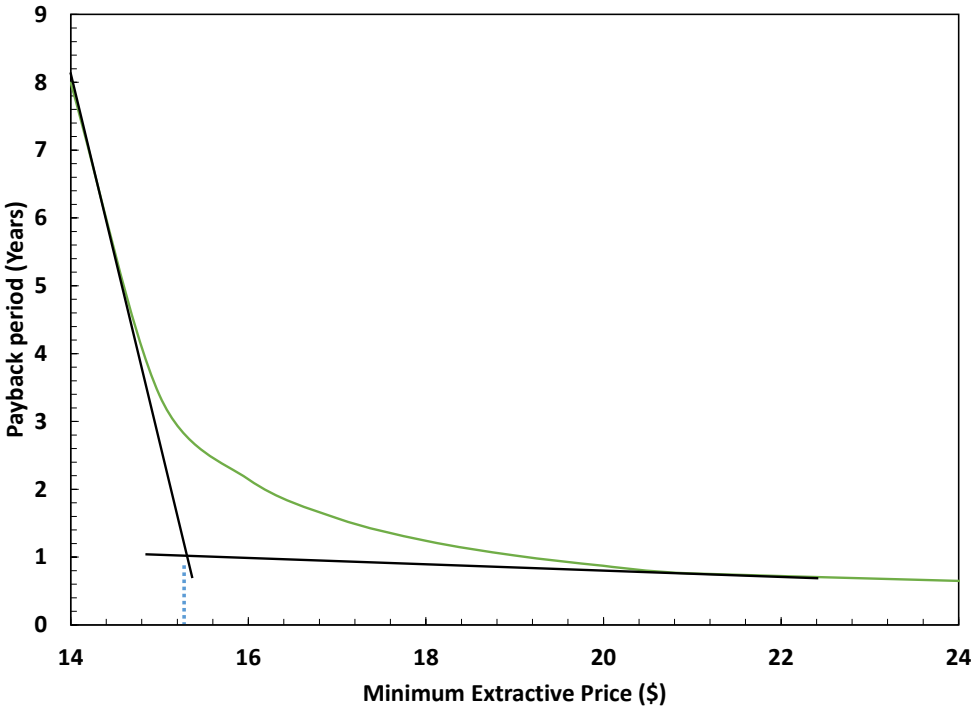

Figure S13. Variation in payback period duration as a function of minimum extractive price. Green line is the line relating payback period with minimum extractive price. The black lines are used to guide the eyes indicating a change in behavior/slope around a MEP of $15.0.

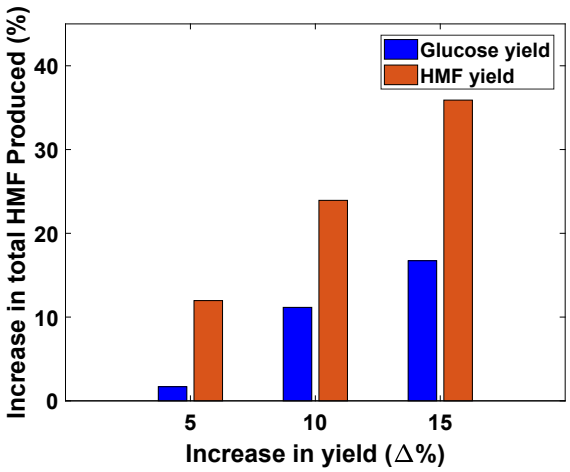

Figure S14. Sensitivity Analysis (SA) for change in yield of glucose and HMF.

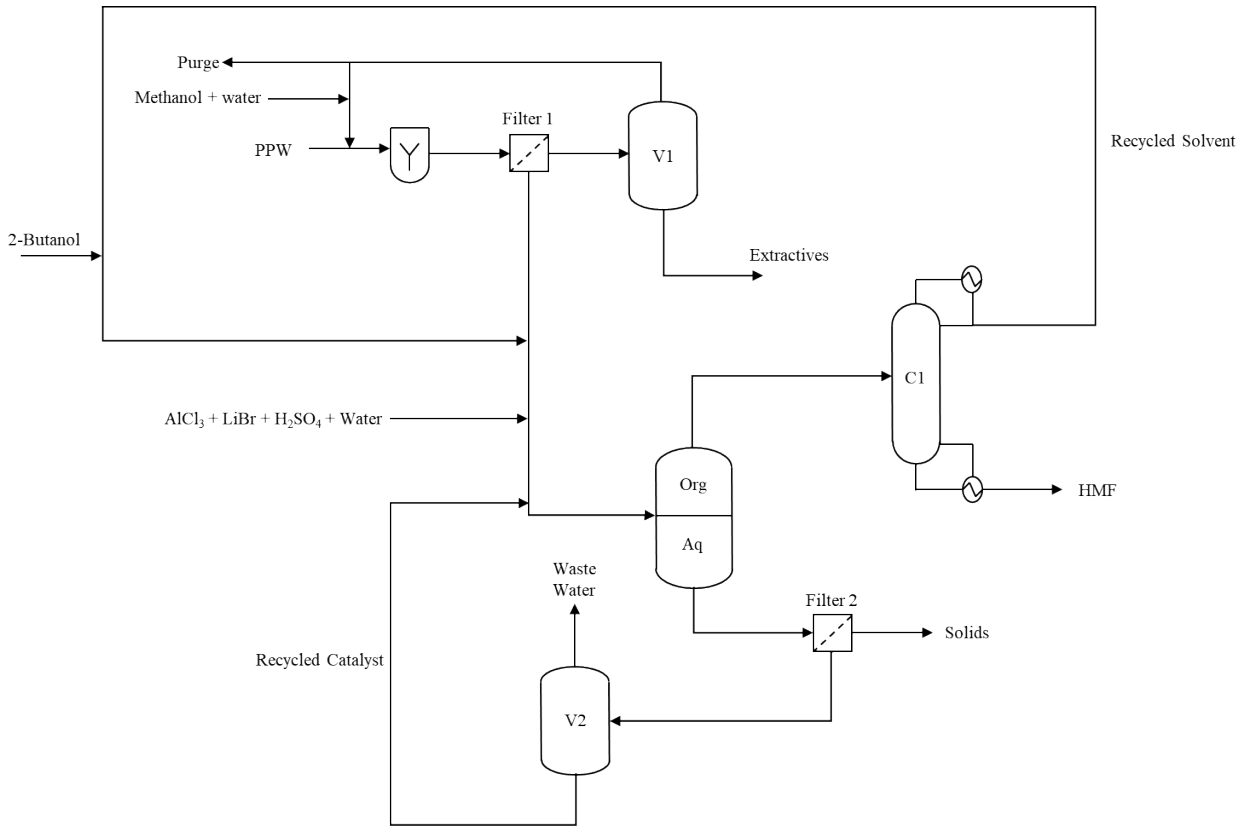

Figure S15. Flowsheet of HMF production from potato peels.

Table S1. Experimental factors levels.

Factors	Levels		
Temperature (°C)	140	150	160
Time (hr)	1	2	3
$AlCl_3$: Glucose mol ratio	0.2	0.5	0.8

Table S2. Complete Box-Behnken design matrix for glucose dehydration.

		Independent variables			Response variables (mol. %)		
Run Order	Blocks	Temperature	Catalyst Concentration	Time	HMF Yield	Fructose Yield	Glucose Conversion
1	2	140	80	2	9.41	20.78	24.56
2	2	150	20	3	27.97	19.56	51.76
3	2	160	20	2	28.54	20.33	47.37
4	2	160	50	1	24.06	22.98	44.1
5	2	150	50	2	27.46	26.01	39.47
6	2	140	20	2	3.45	18.31	8.63
7	2	160	80	2	52.02	10.06	82.18
8	2	140	50	1	8.12	21.19	10.45
9	2	150	50	2	32.73	22.82	56.18
10	2	150	20	1	4.67	16.37	15.49
11	2	150	80	1	10.92	21.57	21.18
12	2	150	80	3	53.04	7.05	87.86
13	2	160	50	3	54.05	2.94	93.84
14	2	150	50	2	28.86	22.28	55.37
15	2	140	50	3	24.51	26.69	48.75
16	1	140	20	2	11.59	23.31	9.58
17	1	160	50	1	30.61	22.56	48.12
18	1	160	20	2	25.98	19.86	45.61
19	1	150	20	3	17.89	16.19	40.9
20	1	150	80	1	10.59	19.12	32.56
21	1	150	50	2	15.08	23.81	31.18
22	1	140	80	2	11.53	20.57	27.33
23	1	140	50	3	19.17	22.83	43.21
24	1	140	50	1	4.45	19.28	15.49
25	1	160	50	3	57.48	3.89	90.48
26	1	150	50	2	35.48	19.42	58.68
27	1	150	80	3	44.32	15.3	73.31
28	1	150	20	1	13.12	27.74	23.47
29	1	160	80	2	54.96	9.89	85.13
30	1	150	50	2	24.97	29.78	28.9

Table S3. Peaks and phenolic compounds in the potato peel waste extracts solution.

Peak Retention time (min)	Compound name	Concentration (µg/ml)
6.65	Peak 1	N/A
6.91	Peak 2	N/A
8.82	Chlorogenic acid	3937±0
9.27	Peak 4	N/A
9.82	Caffeic acid	1286±0
12.02	*p*-coumaric acid	45.1±0
12.66	Ferulic acid	228±0
12.96	Peak 8	N/A
13.24	Peak 9	N/A

Table S4. ANOVA table for Box-Behnken model.

Source	DF	Adj SS	Adj MS	F-Value	P-Value
Model	10	7346.37	734.64	28.16	0
Blocks	1	5.28	5.28	0.2	0.658
Linear	3	6574.37	2191.46	84	0
Temperature	1	3465.88	3465.88	132.85	0
Catalyst Concentration	1	806.59	806.59	30.92	0
Time	1	2301.9	2301.9	88.24	0
Square	3	127.7	42.57	1.63	0.215
Temperature*Temperature	1	9.32	9.32	0.36	0.557
Catalyst Concentration*Catalyst Concentration	1	110.45	110.45	4.23	0.054
Time*Time	1	4.12	4.12	0.16	0.696
2-Way Interaction	3	639.02	213.01	8.16	0.001
Temperature*Catalyst Concentration	1	270.82	270.82	10.38	0.004
Temperature*Time	1	82.86	82.86	3.18	0.091
Catalyst Concentration*Time	1	285.35	285.35	10.94	0.004
Error	19	495.68	26.09		
Lack-of-Fit	15	272.67	18.18	0.33	0.951
Pure Error	4	223	55.75		
Total	29	7842.05			

Table S5. Model summary.

S	R-sq	R-sq(adj)	R-sq(pred)
5.10766	93.68%	90.35%	85.96%

Table S6. Multiple response prediction.

Variable		Setting		
Temperature		160		
Catalyst Concentration		80		
Time		3		
Response	Fit	SE Fit	95% CI	95% PI
HMF Yield	72.76	4.27	(63.83, 81.69)	(58.83, 86.69)

Table S7. Pyrolysis product distribution.

Composition	mol%
CO	48
H_2	51
CO_2	0.2
CH_4	0.2
C_2H_2	Trace

Table S8. Material balances.

Process Step	Stream Name	Mass Flow (kg/hr)
Extraction	Methanol + Water	177,607
	PPW	10,000
	Filter Outlet – Liquid	165,774
	Filter Outlet – Solid	21,834
	Dried Solid	7,637
	V1 – Vapor	177,555
	V1 – Liquid	2,416
	Purge	1.7
Combined hydrolysis and dehydration	LiBr + $AlCl_3$ Mixture	232,709
	2-butanol (new, total)	54.52, 546418
	Reactor - Organic Phase	547,635
	Reactor – Aqueous Phase	239,129
	Filter 2 – Solids	17,473
	Filter 2 – Liquids	221,656
	Recycled Solvent	546,363
	HMF	1,271
	Waste Water	194
	Recycled Catalyst	221,240

Table S9. Utility consumption.

Utility	Load (KJ/hr)
Cooling Water	992,368,237

LP Steam	352,903,920
MP Steam	204,870,413
HP Steam	444,164,413
Fired Heater	62,342,167
Electricity	1806 KW

Table S10. Summary of the capital and operating costs of the HMF process.

Item	**Cost (Million $)**	**Item**	**Cost per year (Million $)**
Total Installed Equipment Cost	45.85	Total Raw Materials Cost	34.6
Other	14.8	Total Utilities Cost	23.8
General and Administrative Overheads	1.7	Operating Labor Cost	0.9
Contract Fee	1.8	Maintenance Cost	1.2
Contingencies	6.06	Operating Charges	0.2
Working Capital	3.5	Plant Overhead	1.06
Total Capital Cost	**73.75**	General and Administrative Cost	4.0
		Total Electricity Sold	3.7
		Total Operating Cost	**62.09**

Table S11. Breakdown of costs.

Process Step	Capital Cost (MM$)	Operating Cost (MM$)
Extraction Step	3.67	0.02
Combined Hydrolysis and dehydration step	15.2	34.59
Pyrolysis	8.83	
Heat exchangers	9.00	
Electricity Production	8.5	
Utilities		23.8
Total Equipment Cost	45.85	
Total Capital Cost	73.75	
Total Operating Cost		62.09

Table S12. REI ratios for different biorefineries

Biorefinery Type	$\frac{Revenue}{E_{Input}}(REI)\frac{\$}{MJ}$
Food Waste	0.0304
Lignocellulose	0.0104
Cellulosic Ethanol	0.0173
Anaerobic Digestion	0.0191

Table S13. Parameters used in computing REI ratios

	Energy Input	Product	Unit price of product	Product Yield	Basis
Lignocellulose	1116000 KJ/s[2]	Cellulose pulp, furfural, lignin	$ 700/ton[2]	700 kg/ ton feedstock[2]	0.0232 ton feedstock/s[1]
Ethanol	81090 KJ/gal[4]	Ethanol	$ 1.4/gal[5]	112 gal/ ton feedstock[4]	0.01 ton of feedstock[2]
Anaerobic Digestion	59400 KJ/ ton feedstock[3]	Biomethane	$ 2.3/1000 ft[6]	492 ft[3]/ ton feedstock[3]	1 ton feedstock[3]

Table S14. Reaction specifications.

Reactions	Hydrolysis	Dehydration	Pyrolysis
Catalyst	LiBr + H_2SO_4	$AlCl_3$	N/A
T (°C)	140	160	1000
P (bar)	1	20	1
Yield (%)	85	40	0

Table S15. Raw material cost.

Raw Material Cost	**Cost ($ per tonne)**
Methanol	518[7]
Aluminium Chloride	600[8]
2-Butanol	988[9]
LiBr	1,400[8]
Sulphuric Acid	125[10]

Table S16. Product cost.

Product Cost	**Cost ($ per tonne)**
Extractives	25,000
HMF	1,000[2]
Bio-Char	2,580[11]

Estimation of extractive price[12]

$$\frac{\$38}{120\ capsule} * \frac{2\ capsule}{770\ mg\ of\ extracts} * \frac{1000\ mg\ of\ extracts}{g\ of\ extracts} = \frac{\$0.82}{g\ of\ extracts} = \frac{\$820}{kg\ of\ extracts}$$

This price even falls within the range ($11.2 - $1120/kg) given in Cristobal *et al*[13] for phenolic extracts.

Considering that we have 30 mg of phenolics (not accounting for flavonoids) per g of PPE, we can further estimate the price for the as-is PPE:

$$\frac{\$820}{kg\ of\ extracts} * \frac{0.03\ g\ phenolics}{1\ g\ of\ PPE} = \frac{\$24.6}{kg\ of\ PPE}$$

We then used $25/kg of extractives for the economic calculations.

This estimated extractive price falls within literature values used by Lane *et al*[14]. Of $ 35/kg and Cristobal *et al*[13]. of $11.2 - $1120/kg.

Evaluation of statistical significance of regression model

The low p-value from the regression analysis (<< 0.05) indicates the significance of the model. The statistical significance of the model was further evaluated using the F-statistic. Since the F-value (28.16) from the ANOVA regression analysis (Figure 4) is much higher than F obtained from the test table (2.98),

the model is considered statistically significant with 95% of confidence. Also, F-test$_{ANOVA}$ was 10 times larger than F-test$_{table}$, satisfying the interpretability multiplier indicating the model's adequacy. The regression coefficient of the model (Table S5) indicates that 94% of the response variability is captured by the model. The residual plots (Figure S4) show no trends in the data set and the distribution of residuals. Only one data point was outside of two standard deviations and none were outside of three standard deviations, which indicates the model describes the data well.

Techno-economics analysis

Using the data from above and some simplifications, a preliminary simulation of the production processes is performed using Aspen Plus®V11. The NRTL method is utilized to predict the liquid-liquid and liquid-vapor behavior. Most of components involved in the reactions are directly selected from the Aspen database, whereas some not included in the database (i.e. components of biomass and humins) are defined by the structures and the properties used by NREL[15]. All the missing parameters are estimated by the molecular structures using the UNIFAC model and the Thermo Data Engine (TDE). TDE is a thermodynamic data correlation, evaluation, and prediction tool developed by the collaboration of Aspen plus and the National Institute of Standard and Technology[16]. The composition of biomass is shown in main text Table 1.

Process description of the integrated FW biorefinery

The biorefinery process (Figure S15) starts with the separation of extractives from the carbohydrates and lignin using a water-methanol mixture. The mixture is mixed using an ultrasonic mixer for 15 minutes at room temperature. The outlet stream from the mixer is introduced to a filter to remove the extractant and the solid mixture. A series of flash drums is used to separate methanol and to dry the extractives for a purity of 95%. The solid mixture is first dried and then mixed with water containing LiBr, $AlCl_3$ and H_2SO_4 and then introduced to a reactor for hydrolysis at a temperature of 140 ^oC for a residence time of 1 hr. After hydrolysis, the product mixture is mixed with a 2-butanol and introduced in a "one-pot" reactor where simultaneous dehydration reaction and separation of HMF occurs at 160 ^oC and 20 bar for a residence time of 3 hrs. 80% of the HMF is extracted by the organic phase and is sent to a distillation column for purification. The solvent is recycled. The aqueous phase is filtered to remove the unreacted solids and humins. The liquid phase is then flashed to remove excess water and the liquid is recycled back to the dehydration reactor. The solid phase is used to produce bio-char by pyrolyzing it at 1000 ^oC. Pyrolysis was simulated as close to the literature data and the pyrolysis gases consist of mostly CO and H_2 with trace amount of CO_2, CH_4 and C_2H_2 and biochar as the main product. The gas is then used to generate electricity and both the capital costs and the operating costs are included. The cost of pollutant control is assumed in the total cost of the pyrolysis reactor. The gas after electricity production consists of CO_2 and H_2O.
For the process simulation, the following assumptions are made:

1. Filtration processes to separate extractives, carbohydrates and unreacted biomass from the combined hydrolysis and dehydration process are assumed to have 95% separation efficiency.
2. The byproducts do not affect the conversion and selectivity of any reactions. No separation steps are considered before hydrolysis.
3. There is no mixing between the organic and aqueous phases.
4. Reaction details are given in Table S14.

The capacity of the process to produce HMF is based on processing of 80,000 metric ton of PPW per year. The total production of HMF is 1,271 kg/hr or 10,171 metric tons per year, extractives is 2,416 kg/hr or 19,326 metric tons per year and bio-char is 469 kg/hr or 3,749 metric tons per year. The concentration of PPW in the mixture is ~4 wt.% and the amount of solvent needed for the extraction in the dehydration reaction increases the overall volume of the process which in turn increases the cost of capital and the utility cost. 96% of the total raw material cost is because of the cost of LiBr.

Assumptions for TEA

1. Plant capacity is assumed as 10 metric tons per hour of dry potato peels feedstock.

2. All the equipment and operating costs estimated by Aspen Economic Analyzer V11 are based on the price of the first quarter in 2018. The filtration units are not explicitly designed, and the design is based only on the flowrates.
3. The cost of the peels is taken as zero.
4. The plant operates in a continuous mode for 8,000 hr per year. The economic life of the project is assumed to be 20 years. 15% per year interest rate is applied to the capital cost. 35% corporate tax is applied to the profits. The simplest depreciation method – the straight-line method is applied as the salvage value – is 10% of the original capital cost after 20 years. The recovery period is considered as 10 years.
5. The market price of the raw materials is given in Table S15.
6. The market price of the products is given in Table S16.
7. The cost of the ultrasonic mixer was estimated by adding the cost of a static mixer and a 100–300 kW ultrasound[17] ($2.8 million). The cost of the pyrolysis reactor ($8.83 million) was estimated using the sizing curve developed for pyrolysis plants by Brammer *et al*[18] and calculated for the year 2018 using the chemical engineering plant cost index[19].
8. Heat integration is carried out using the Aspen Energy Analyzer® V11, which uses the pinch analysis method for heat integration. The lowest operating cost scenario is considered for heat integration. All the utilities are purchased, and wastewater is treated by a third party at a fixed price per unit volume[20].
9. Three profitability metrics were calculated (Equations S1 – S6)[13] to evaluate the feasibility of the biorefinery: return on Investment (ROI), payback time, and breakeven.
10. The ROI is the ratio of gains to cost and it measures (in %), per period, the rate of return on money invested in the biorefinery. A positive ROI means that the investment gains compare favorably to the costs; the larger the ROI, the better. The payback time is the time needed for the gains from the investment to equal the costs, i.e., for an investment to pay for itself. The smaller the payback time, the better. Breakeven refers to the specific period in which it's the profits from an investment equal its total costs and its net income will be zero.

$$ROI = \frac{Annual\ net\ profit}{Total\ capital\ investment} \quad \text{(Eq. S1)}$$

$$Payback\ Time = \frac{Total\ capital\ investment}{Annual\ net\ profit} \quad \text{(Eq. S2)}$$

$$Break\ Even\ (units) = \frac{Fixed\ Cost}{\left(\frac{Price}{unit} - \frac{Variable\ cost}{unit}\right)} \quad \text{(Eq. S3)}$$

$$Depreciation = \frac{(Capital\ Cost - Salvage\ Value)}{Recovery\ Period} \quad \text{(Eq. S4)}$$

$$Net\ Profit = Revenue - (Corporate\ Tax + Depreciation + Interest + Operating\ cost) \quad \text{(Eq. S5)}$$

$$Fixed\ Cost = Utilities\ Cost + Depreciation + Interest \quad \text{(Eq. S6)}$$

References

(1) Food and Agriculture Organization of the United Nations. FAOSTAT http://www.fao.org/faostat/en/#data/QC (accessed May 8, 2019).

(2) Alonso, D. M.; Hakim, S. H.; Zhou, S.; Won, W.; Hosseinaei, O.; Tao, J.; Garcia-Negron, V.; Motagamwala, A. H.; Mellmer, M. A.; Huang, K.; Houtman, C. J.; Labbé, N.; Harper, D. P.; Maravelias, C. T.; Runge, T.; Dumesic, J. A. Increasing the Revenue from Lignocellulosic Biomass: Maximizing Feedstock Utilization. *Sci. Adv.* **2017**, *3* (5). https://doi.org/10.1126/sciadv.1603301.

(3) Ministry of Agriculture and Food and Rural Affairs. Energy Yields from a Farm-Based Anaerobic Digestion System http://www.omafra.gov.on.ca/english/engineer/facts/enyields.htm#6 (accessed Sep 11, 2019).

(4) Lorenz, D.; Morris, D. *How Much Energy Does It Take to Make a Gallon of Ethanol?*; Minneapolis,

1992.

(5) U.S. GRAINS COUNCIL. Ethanol Market and Pricing Data - February 19, 2019 - U.S. GRAINS COUNCIL https://grains.org/ethanol_report/ethanol-market-and-pricing-data-february-19-2019/ (accessed Sep 11, 2019).

(6) MacroTrends. Natural Gas Prices - Historical Chart | MacroTrends https://www.macrotrends.net/2478/natural-gas-prices-historical-chart (accessed Sep 11, 2019).

(7) Methanex. Methanex Methanol Price Sheet https://www.methanex.com/sites/default/files/methanol-price/Mx-Price-Sheet - Feb 28%2C 2019.pdf (accessed Mar 7, 2019).

(8) Sadula, S.; Athaley, A.; Zheng, W.; Ierapetritou, M.; Saha, B. Process Intensification for Cellulosic Biorefineries. *ChemSusChem* **2017**, *10* (12), 2566–2572. https://doi.org/10.1002/cssc.201700183.

(9) Alibaba. 2 Butanol Price, Wholesale & Suppliers - Alibaba https://www.alibaba.com/showroom/2-butanol-price.html (accessed Mar 7, 2019).

(10) US Producer Price Index: Chemicals and Allied Products: Sulfuric Acid https://ycharts.com/indicators/us_producer_price_index_chemicals_and_allied_products_sulfuric_acid_yearly (accessed Mar 17, 2020).

(11) Porter, P.; Laird, D. Biochar: Prospects of Commercialization https://articles.extension.org/pages/71760/biochar:-prospects-of-commercialization (accessed Mar 7, 2019).

(12) Super Antioxidants Veg Capsules | NOW Foods https://www.nowfoods.com/supplements/super-antioxidants-veg-capsules (accessed Jan 4, 2020).

(13) Cristóbal, J.; Caldeira, C.; Corrado, S.; Sala, S. Techno-Economic and Profitability Analysis of Food Waste Biorefineries at European Level. *Bioresour. Technol.* **2018**, *259* (January), 244–252. https://doi.org/10.1016/j.biortech.2018.03.016.

(14) Lane, J. Unorthodox antioxidant focus drives Stover Ventures towards cellulosic dream : Biofuels Digest http://www.biofuelsdigest.com/bdigest/2018/08/22/unorthodox-antioxidant-focus-drives-stover-ventures-towards-cellulosic-dream/ (accessed Sep 27, 2018).

(15) Humbird, D.; Davis, R.; Tao, L.; Kinchin, C.; Hsu, D.; Aden, A.; Schoen, P.; Lukas, J.; Olthof, B.; Worley, M.; Sexton, D.; Dudgeon, D. *Process Design and Economics for Biochemical Conversion of Lignocellulosic Biomass to Ethanol: Dilute-Acid Pretreatment and Enzymatic Hydrolysis of Corn Stover*; Colorado, 2011.

(16) Lin, Z.; Nikolakis, V.; Ierapetritou, M. Alternative Approaches for p-Xylene Production from Starch: Techno-Economic Analysis. *Ind. Eng. Chem. Res.* **2013**, *53*, 10688–10699. https://doi.org/10.1021/ie402469j.

(17) Bussemaker, M. J.; Day, K.; Drage, G.; Cecelja, F. Supply Chain Optimisation for an Ultrasound-Organosolv Lignocellulosic Biorefinery: Impact of Technology Choices. *Waste and Biomass Valorization* **2017**, *8* (7), 2247–2261. https://doi.org/10.1007/s12649-017-0043-6.

(18) Rogers, J. G.; Brammer, J. G. Estimation of the Production Cost of Fast Pyrolysis Bio-Oil. *Biomass and Bioenergy* **2012**, *36*, 208–217. https://doi.org/10.1016/j.biombioe.2011.10.028.

(19) Chemical Engineering Plant Cost Index: 2018 Annual Value - Chemical Engineering | Page 1 https://www.chemengonline.com/2019-cepci-updates-january-prelim-and-december-2018-final/ (accessed Mar 17, 2020).

(20) Kazi, F. K.; Patel, A. D.; Serrano-Ruiz, J. C.; Dumesic, J. A.; Anex, R. P. Techno-Economic Analysis of Dimethylfuran (DMF) and Hydroxymethylfurfural (HMF) Production from Pure Fructose in Catalytic Processes. *Chem. Eng. J.* **2011**, *169* (1–3), 329–338.

https://doi.org/10.1016/j.cej.2011.03.018.